Published in final edited form as:
Biomaterials. 2013 January ; 34(2): 331–339. doi:10.1016/j.biomaterials.2012.09.048.

Application of Visible Light-based Projection Stereolithography for Live Cell-Scaffold Fabrication with Designed Architecture

Hang Lin, **Dongning Zhang**, **Peter G. Alexander**, **Guang Yang**, **Jian Tan**, **Anthony Wai-Ming Cheng**, and **Rocky S. Tuan***
Center for Cellular and Molecular Engineering, Department of Orthopaedic Surgery, University of Pittsburgh School of Medicine, Pittsburgh, Pennsylvania 15219, USA

Abstract

One-step scaffold fabrication with live cell incorporation is a highly desirable technology for tissue engineering and regeneration. Projection stereolithography (PSL) represents a promising method owing to its fine resolution, high fabrication speed and computer-aided design (CAD) capabilities. However, the majority of current protocols utilize water-insoluble photoinitiators that are incompatible with live cell-fabrication, and ultraviolet (UV) light that is damaging to the cellular DNA. We report here the development of a visible light-based PSL system (VL-PSL), using lithium phenyl-2,4,6-trimethylbenzoylphosphinate (LAP) as the initiator and polyethylene glycol diacrylate (PEGDA) as the monomer, to produce hydrogel scaffolds with specific shapes and internal architectures. Furthermore, live human adipose-derived stem cells (hADSCs) were suspended in PEGDA/LAP solution during the PSL process, and were successfully incorporated within the fabricated hydrogel scaffolds. hADSCs in PEG scaffolds showed high viability (>90%) for up to 7 days after fabrication as revealed by Live/Dead staining. Scaffolds with porous internal architecture retained higher cell viability and activity than solid scaffolds, likely due to increased oxygen and nutrients exchange into the interior of the scaffolds. The VL-PSL should be applicable as an efficient and effective tissue engineering technology for point-of-care tissue repair in clinic.

Keywords

Adipose-derived stem cells; Projection stereolithography; Lithium phenyl-2,4,6-trimethylbenzoylphosphinate; Polyethylene glycol; Scaffold fabrication

1. Introduction

Biomaterial scaffolds represent a critical component in tissue engineering and regenerative medicine [1]. Some of the desired tissue engineering requirements for scaffolds include biocompatibility, biodegradability and suitable mechanical stiffness that together allow cell/tissue growth, integration and remodeling [2]. An ideal scaffold should also permit fabrication of customized shapes to accurately mimic native tissue structures or to completely fill in the injury defects, as well as possess appropriate internal micro-

*Correspondence: Rocky S. Tuan, PhD, Center for Cellular and Molecular Engineering, Department of Orthopaedic Surgery, University of Pittsburgh School of Medicine, 450 Technology Drive, Room 206, Pittsburgh, PA, 15219, USA, Phone: 4126482603, Fax: 4126245544, rst13@pitt.edu.

architecture to facilitate cell/tissue growth. Studies have suggested that scaffolds with internal space are more compatible for tissue engineering in terms of cell retention and viability than solid scaffolds, with different pore size and shapes for different tissues [3, 4]. For example, the reported optimal scaffold pore sizes for engineered bone are 100 – 500 μm [5], and only 20-50 μm for engineered cartilage [6]. Among the various modeling methods, solid free form fabrication (SFF) promises the greatest ability to precisely control the geometry of scaffolds based on computer-aided design (CAD)-generated 3-dimensional (3D) models or clinical images [3]. At present, major SFF techniques employed in tissue engineering include selective laser sintering, plotting, 3D printing and stereolithography, the first SFF technique developed, which remains the most accurate [7]. The principle of stereolithography is based on the photopolymerization of derivatized monomers, e.g., containing vinyl groups, triggered by free radicals that are produced from photoinitiators upon exposure to either UV or visible light [8]. 3D scaffolds are then formed by controlled solidification at defined sites on a movable building platform [9].

Stereolithographic techniques using digital light processors (DLP) and projectors, termed projection stereolithography (PSL), are receiving increased attention owing to their high fabrication rate and resolution. Such characteristics are accomplished through the projection of an entire image by masked illumination upon the monomer solution to simultaneously form an entire layer, thus greatly reducing fabrication time [7]. To control the structure of scaffolds using PSL, 3D models from computer-aided design (CAD) or clinical images are first sliced sequentially into a series of cross-sectional images with defined thickness (often 25-100 μm). Upon projection to the monomer solution, one layer of polymer is produced for each image projection. Sequential projection in layers results in fabrication of the specified 3D structures. Together, these features give this technique its high resolution and flexibility.

Scaffolds derived from different materials with different properties and structures have been fabricated using PSL [10-12]. Currently, most photoinitiators applied in PSL are not water-soluble and must be dissolved in organic solvents. Due to the cellular toxicity of organic solvents, such photoinitiators cannot be used to construct live cell-included scaffolds. In addition, the use of UV light for curing carries the risk of generating double-strand DNA breaks in the encapsulated cells [13]. Therefore, in most studies using this technique, cells are seeded onto the scaffolds after fabrication, rather than incorporated within the scaffold during fabrication. As a result, cell seeding is often incomplete and inefficient [14]. These problems greatly limit the application of PSL in live-cell scaffold fabrication.

In order to achieve complete and uniform distribution of live cells within a scaffold, a visible light based PSL (VL-PSL) system with live-cell fabrication ability is desired (Figure 1). In developing such a system, three major factors need to be taken into consideration. First, visible light and a visible light-activated initiator must be used. The ideal visible light-activated initiator should be water soluble and non-cytotoxic while retaining rapid and efficient radical production. Second, the cells must remain uniformly suspended in the monomer/initiator solution during PSL fabrication. Third, the scaffold itself must be non-cytotoxic and hydrophilic to maintain cell viability after cell encapsulation. Hydrogels are thus suitable as they are capable of trapping water, and their physical properties can mimic those of living tissues [15].

In this study, we used a combination of polyethylene glycol diacrylate (PEGDA) and lithium phenyl-2,4,6-trimethylbenzoylphosphinate (LAP) [16] to fabricate hydrogel scaffolds faithfully from CAD-generated 3D models using VL-PSL. Human adipose-derived stem cells (hADSCs) and Insulin-Transferrin-Selenium (ITS) were also included into the PEG/LAP solution and then incorporated into scaffolds during the PSL process. We tested the cytotoxicity of PEG/LAP solution in short and long term culture with hADSCs.

Furthermore, cell viability and bioactivities in solid and porous scaffolds were analyzed and compared by Live/Dead assay and MTS assay up to 7 days after fabrication. Our results clearly demonstrated the successful fabrication of PEG hydrogels with designed geometries and internal architectures using VL-PSL, and the efficient encapsulation of cells that retained high and long-term viability.

2. Materials and methods

2.1. Materials

All chemicals used in these experiments were purchased from Sigma-Aldrich (St. Louis, MO) unless stated otherwise. The visible light sensitive initiator lithium phenyl-2,4,6-trimethylbenzoylphosphinate (LAP) was synthesized as described by Fairbanks et al. [16]. Briefly, dimethyl phenylphosphonite was reacted with 2,4,6-trimethylbenzoyl chloride for 18 hours. The product LAP was precipitated by adding 2-butanone, washed with 2-butanone for 3 times, and then vacuum-dried and stored dessicated at room temperature.

2.2. PEGDA preparation

Briefly, 5 g PEG (4kd, Fluka, Milwaukee, WI) was dissolved in 15 ml anhydrous dicholoromethane (DM) followed by the addition of 0.44 ml methacrylic anhydride (MA), 0.25 ml triethylamine (TEA) and 3 g molecular sieves. After thorough mixing, the solution was protected from light and allowed to react for 4 days at room temperature. The final PEGDA suspension was filtered to remove the solvent and dried overnight under high vacuum. The dried PEGDA was then dissolved in H_2O at 30% concentration (w/v) and dialyzed against H_2O to completely remove all low-molecular-weight contaminants using 2000 NMWCO dialysis tubing (Sigma-Aldrich).

2.3. Initiator screening using PSL apparatus

The PSL apparatus was purchased from EnvisionTec (Perfactory Standard, Gladbeck, Germany) equipped with digital light processing (DLP) technology. All fabrications in this study were done using the visible light mode (Hg illumination with UV barrier filter). The depth of each layer was set at 50 μm. The material used for PSL scaffold fabrication was composed of 10% (w/v) PEGDA in H_2O. All initiators used in this study were summarized in Table 1 [17-27].

The water solubility of candidate initiators was first tested at 0.1% (w/v). The water-soluble initiators were then mixed with 10% PEGDA at different concentrations, and the mixtures were used as the starting materials for PSL. The fabricated products by PSL were then compared to the original 3D model (solid cubic structure). The initiators capable of yielding intact and morphologically correct scaffold were applied in subsequent experiments.

2.4. Cell-free Scaffold fabrication by PSL using PEGDA

The material used for PSL scaffold fabrication was composed of 10% (w/v) PEGDA in H_2O or Hank's Balanced Salt Solution (HBSS, Invitrogen) with concentrations of LAP ranging between 0.1-0.6% (w/v).

3D models with different shapes were generated using Magics 14 software (Materialise Leuven, Belgium), including hollow cylindrical, hemispherical, cubical, and pyramidal structures as well as alphanumeric forms. To test the ability of the PSL system to control the internal architectures, 3 models were designed as shown in Figure 3A, B, C, and D. Figure 3A showed a solid structure and Figure 3B-D showed two porous structures. The micropores in the porous-1 models were designed as 500 μm diameter tubes passing top-to-bottom through the structure. The distance between the closest edges of any two tubes was 1 mm.

Figure 3C shows the porous-2 3D model, designed using intersecting beams of 150 μm × 150 μm in height and width spaced such that the resulting pore size was 300 μm×300 μm square.

2.5. hADSCs isolation

hADSCs were isolated from the lipoaspirate obtained from a 28-year-old female with Institutional Review Board approval (University of Pittsburgh) using an automated cell isolation system from Tissue Genesis, Inc (Honolulu, HI). hADSCs were cultured in growth medium (GM: DMEM-high glucose, 10% fetal bovine serum (FBS), 100 units/ml penicillin, 100 μg/ml streptomycin, Invitrogen, Carlsbad, CA). At 80% confluence, cells were detached with 0.25% trypsin in 1 mM EDTA (Invitrogen) and passaged. All experiments were performed with passage 3 (P3) hADSCs.

2.6. LAP toxicity test with hADSCs

hADSCs were seeded on a 24-well plate (Falcon, Becton Dickinson, Lincoln Park, NJ) at 10,000 cells/well and cultured for 24 hours in GM. For short-term toxicity test, the medium was completely removed and 500 μl of HBSS with different LAP concentrations ranging between 0.016% and 1% (w/v) were added to the cultures. Cells were exposed to LAP for 0.5, 1, 2 or 5 hours, at which time the LAP solution was replaced with fresh GM and the culture continued for an additional 3 days.

For long term toxicity tests, the medium was removed and replaced with 500 μl of GM containing LAP at concentrations ranging from 0.016% to 1% (w/v). Cells were cultured in the LAP-containing medium for 3 days.

In both experiments, cell viability was estimated using MTS assay (CellTiter 96 Aqueous Cell Proliferation assay, Promega, Madison, WI) performed according to the manufacturer's instructions.

2.7. hADSCs suspension in PEGDA solution with Percoll

To prevent cell settling during PSL fabrication, Percoll (Sigma-Aldrich) was employed in PEGDA/LAP working solution. Using a 1:10 dilution of Percoll as a stock solution (PSS), a discontinuous gradient of Percoll solutions ranging from 10%-90% (v/v), all prepared in 10% PEGDA/HBSS working solution, was created in a 15 ml conical tube (9 layers of 1 ml each). hADSCs in HBSS (1 ml of 1×10^6 cells/ml) was placed on the top of the gradient, followed by centrifugation at 200 × g for 5 minutes. The Percoll gradient was then fractionated from top to bottom into 1 ml fractions, and cell number in each fraction was determined microscopically. The Percoll concentration of the fraction with the highest cell number was used in subsequent experiments to suspend hADSCs during the PSL process.

2.8. Live-cell scaffold fabrication by PSL using PEGDA containing hADSCs

The monomer solution for live-cell PSL was prepared by mixing 18 ml PSS with 30 ml of 16% PEGDA solution (w/v, in HBSS) followed by adding 0.096 g LAP (0.2%, w/v) and 1× Insulin-Transferrin-Selenium (ITS, Invitrogen). After LAP was completely dissolved, hADSCs were added into the PEGDA/LAP/Percoll solution at a final concentration of 1×10^6 cells/ml. The cell-laden monomer solution was immediately poured into the basement plate in the PSL device, and live-cell PEG scaffolds were produced using CAD derived solid ring, hexagonal and porous-1 structure.

2.9. Live/Dead viability assay of hADSCs in scaffolds produced by PSL

Cell seeded PEG hydrogels scaffolds with solid and porous structure were washed twice with HBSS and cultured in GM (> 4× volume of scaffolds) for up to 7 days. At 1 and 7 days post-fabrication, cell viability was assessed with the Live/Dead Cell Viability Assay (Invitrogen) as examined by epifluorescence microscopy. The percentage of live cells was calculated as the number of green-staining cells divided by the total number of cells.

2.10. MTS assay of hADSCs in scaffolds produced by PSL

PEG hydrogels cylinders (5 mm diameter, 5mm height) were cut from the solid or porous-1 live cell-scaffolds fabricated by PSL using a biopsy punch (Sklar, West Chester, PA). These cylinders were cultured in growth medium in a 24-well plate (1 cylinder in 1 ml GM/well), with the medium being changed every 3 days. After culture day 0 (immediately after scaffold fabrication), 3 and 7, relative bioactivities of the cell-containing cylinders were determined using MTS assay (CellTiter 96 Aqueous Cell Proliferation assay, Promega).

2.11. Statistical Analysis

Each study was carried out with 3 experimental replicates and the results were expressed as the mean ± SD. Statistically significant differences were determined by two-tailed Student's t-test for two-group comparisons or one-way ANOVA for multiple-group comparisons. Significance levels were set at $p<0.05$(*) and $p<0.01$(**).

3. Results

3.1. Initiator screening

10% PEGDA in water was used as the monomer solution to screen the potential photoinitiators for water solubility, light sensitivity and crosslinking effectiveness using visible light PSL. As shown in Table 1, most commercial initiators activated by visible light, such as camphorquinone and Irgacure 784, were soluble in ethanol or DMSO but insoluble in water. Irgacure 2959, the widely used initiator for UV photocrosslinking hydrogels with cell encapsulation, showed some water solubility but failed to be activated to produce free radicals by visible light from our PSL device. Eosin Y with triethanolamine and 1-vinyl-2-pyrrolidinone (ETV) showed some promise, but ETV in PEG solution required long exposure time for hydrogel formation, making it ineffective in the context of our PSL device. Lithium phenyl-2,4,6-trimethylbenzoylphosphinate (LAP), synthesized from dimethyl phenylphosphonite and 2,4,6-trimethylbenzoyl chloride via a Michaelis–Arbuzov reaction [16], showed high solubility in water (up to 1% w/v). Among all candidate initiators tested, only LAP was able to produce PEG hydrogel scaffolds in visible light mode of our PSL device when being dissolved in water at 0.2% (w/v). Therefore, LAP was selected as the photo-initiator in the following experiments.

3.2. PEG scaffolds fabricated by PSL with LAP as the initiator

In order to examine the effect of LAP (0.5%, w/v) as an initiator for PSL scaffold fabrication, PEG hydrogel scaffolds with different shapes were built (Figure 2A). More complicated alphanumeric structures could also be produced (Figure 2B). Based on the measurement of the final polymerized scaffold dimension, the average dimensional difference between the 3D models and actual scaffolds produced by PSL was less than 2% based on direct measurements.

Because the PSL device used in this study employs a projector to deliver light to monomer solution, the minimum dimensions of the final scaffolds depend on the resolution of the projector. In theory, the size of smallest pixel produced by our projector is 70 μm × 70 μm.

Figure 2C&D show the typical surface texture of PEG scaffolds fabricated by PSL. Based on the measurements of voxel dimensions in Figure 2D, the size of the smallest dot is about 68-73 μm square, illustrating the high fidelity of our protocol.

3.3. Fabrication of solid and porous scaffolds by PSL with different LAP concentration

Operating at the maximum resolution of the device, we needed to determine the optimal concentration of LAP required polymerizing different structures. To achieve this goal, we designed one solid rectangle model and two others with different micropore arrangements (Figure 3A-D). The porous-1 design included pores formed by creating voids, 500 μm in diameter, through the y-axis (Figure 3B). The lattice-like porous-2 structure was designed using intersecting beams, 150 μm × 150 μm in height and width, spaced such that the resulting pore size was 300 μm × 300 μm (Figure 3C&D).

In comparing the final geometry of the polymerized PEG scaffolds (Figures 3E-H) to the CAD designs (Figure 3B), we found that a low concentration of LAP, 0.2%, was required for faithful 3D reproduction of the porous-1 design. As we increased the LAP concentration, the tube diameter decreased, increasing the distance between any two tubes (Figure 3E-H). At LAP concentrations greater than 0.5%, superfluous structures outside the defined boundaries of the CAD form were created (data not shown) due to excess free radical production and diffusion. In the production of porous-2 structure, 0.6% LAP was required for accurate replication of the CAD design (Figure 3J). At 0.4% LAP, it appeared that the individual layers formed during fabrication were not strong enough to support stacking of the subsequent layers, resulting in a collapsed and incomplete structure (Figure 3I).

3.4. LAP cytotoxicity test on hADSCs

LAP cytotoxicity at different concentrations was estimated in both short- and long-term culture. Given that during PSL cells were transiently exposed to high concentrations of LAP, which was then rapidly leached into the culture medium afterwards, we first examined short-term LAP toxicity by pre-culturing hADSCs in LAP solution at a series of concentration for up to 5 hours. As shown in Figure 4A, cell viability was not significantly affected by LAP concentrations below 0.5%. These results were confirmed by microscopic examination of cell morphology (data not shown). Thus, hADSCs were able to tolerate 0.5% LAP in HBSS solution for up to 5 hours without obvious cell death, a time period sufficient for producing scaffolds up to 25 mm in height.

To further investigate the long term effect of LAP exposure on cell viability, hADSCs were cultured in growth medium with different LAP concentrations for 3 days. As shown in Figure 4B, cell viability was significantly decreased when LAP concentration in the medium was greater than 0.0625%. Thus, culturing fabricated PEG hydrogels in a sufficient volume of medium was critical to ensure maximal cell survival post-fabrication.

3.5. Application of Percoll to prevent hADSCs sedimentation during PSL

Uniform cell distribution throughout the scaffold is one of the desired characteristics of our process. Because hADSCs rapidly settled to the bottom of the monomer solution, we included an optimized concentration of Percoll in PEG/LAP solution to match the buoyant density of the cells to keep them suspended. As shown in Figure 5, most of cells stayed in the layers with 30% and 40% Percoll. We then refined our density test using 25-45% Percoll, and confirmed that 37.5% Percoll (specific gravity of 1.0496) was most efficient for hADSCs suspension (data not shown). This Percoll concentration was then used in all subsequent experiments.

3.6. Assessment of cell viability of hADSCs incorporated into PSL-fabricated PEG hydrogel by Live/Dead staining

The calcein acetoxymethyl (calcein-AM)/ethidium homodimer-1 (EthD-1) based Live/Dead cell viability assay was used to assess cell viability (Figure 6; green staining = live cells, red staining = dead cells). A high percentage of viable cells (>95%) was seen in both solid and porous scaffolds 24 hours after fabrication (Figure 6A-H). The cells retained their round shape, and were evenly distributed within the fabricated scaffolds accordingly, including ring and hexagonal structures (Figure 6A-D), even around the pores (Figure 6I&J). A lateral view revealed that cells were uniformly distributed from top to bottom of the solid scaffold (Figure 6K). After 7 days of culture in GM, hADSCs retained a high rate of viability (>90%) not only on the surface of the constructs but in the different layers in the scaffolds as well (Figure 7).

3.7. MTS cell viability assay of hADSCs incorporated into PSL-fabricated PEG hydrogel

In a separate, parallel set of samples, we compared hADSCs viability in solid versus porous-1 scaffolds at different time points over a 7-day period, using MTS assay to measure cellular metabolic activity (Figure 8). We observed that immediately after fabrication (day 0), cell activities were the same in both solid and porous structures. However, at day 3, a significant increase in cell activity was observed in the porous structures compared to the solid structure. This difference decreased but was still significant at day 7.

4. Discussion

Live cell-scaffold fabrication is one of the key technologies used to engineer tissues in vitro or to create grafts for tissue regeneration in vivo. We report here the development of a VL-PSL technology for the incorporation of live hADSCs into the PEGDA solution during scaffold fabrication and the maintenance of high cell viability in the scaffolds for up to 7 days. With computer-aided design, PEG scaffolds with different geometries and internal architectures were produced via VL-PSL with high fidelity. The high resolution of the system was used to create structures with micropores, in which encapsulated hADSCs showed higher bioactivity than in solid scaffolds.

Successful scaffolds for tissue engineering need to reproduce accurately the native tissue structures [28]. Stereolithography represents one of the most promising fabrication methods, capable of building objects at an accuracy of 20 μm [7]. At present, stereolithography fabrication technologies include two main types, projection stereolithography (PSL) and laser stereolithography (LSL). Compared to LSL that uses a point-by-point laser scanning procedure [29], PSL builds an entire layer with one single exposure and therefore substantially reduces fabrication time. However, most commercially available monomer solutions for use in PSL do not support or prevent cell growth, severely limiting the application of PSL in tissue engineering. To overcome this limitation, many biodegradable materials capable of supporting cell growth have been adapted for PSL, including synthesized polymers such as poly(trimethylene carbonate) [11], poly(ethylene glycol)/poly(D,L-lactide) [12], and naturally derived polymers, such as gelatin [10]. However, in most studies, live cells are not included during the PSL process, such that scaffold fabrication and cellularization are performed in two separate steps. Post-fabrication seeding often results in uneven and incomplete cell distribution through the construct [10, 30]. To overcome this, cell seeding devices have been used to force the cells into the scaffolds by pressure-assisted perfusion or vacuum [31]. Even with these methods, cells were still often observed to reside and grow only on the available surfaces of the construct rather than within the scaffolds, thus increasing scaffold remodeling time and resulting in uneven tissue regeneration.

One approach to achieve uniform cell distribution within a construct is to mix the cells with the monomer during the fabrication process. The aim of this investigation was to develop a PSL system capable of including live cells in the low cytotoxicity monomer solution during fabrication to enable spatially-controlled cell distribution inside the scaffolds. To achieve this goal, we needed to consider all the factors involved in PSL, including materials, light source, initiator and cells.

We first chose hydrogel materials that not only can incorporate cells but also retain sufficient aqueous medium in the scaffold to support cell growth during and after the fabrication process. Hydrogel scaffolds have been shown to perform well in certain cases of tissue repair, such as cartilage [32]. However, their use is restrained by the limited technologies available to produce complex internal architectures [33]. In our study, PEG hydrogel was used because it is easily prepared, water-soluble, and non-cytotoxic [34]. To date, encapsulation of live cells in PEG scaffolds using LSL has been reported with UV light and I2959 as the initiator, but long-term cell viability was either not determined [35] or reported to be < 50% after 2 weeks [36]. The poor cell viability could be the result of repeated exposure to UV light during fabrication and the cytotoxicity of I2959 [37]. We thus chose to use visible light as the light source.

For the purpose of VL-PSL, we screened several commonly available initiators. Eosin Y, the first visible light initiator applied in tissue engineering [38], can be dissolved in water but has limited efficiency. Results indicated that only LAP showed high polymerization efficiency (>I2959) and low cytotoxicity [16]. We observed that high cell survival was possible after 5 hour exposure to LAP at concentrations as high as 0.5 % (Figure 4). These features (visible light activation, high efficiency for rapid polymerization and fabrication, and low cytotoxicity) were all critical factors in the selection of LAP as the initiator of choice for live-cell PSL.

By the VL-PSL developed in this study, PEG scaffolds with different architectures were successfully produced. It took about 30 minutes to produce scaffolds with 2 mm in height. Because PEG hydrogel is clear, we noticed that visible light is able to pass through the scaffolds and crosslink previously cured layers, which results in extra structures. Phenol Red and Orasol Orange G have been applied to deal with this problem in acellular scaffold fabrication using visible-light PSL [11, 12]. Future studies will test the inclusion of such reagents to increase the Z-axis fidelity of our system.

In our initial experiments, we found that cells rapidly sedimented in the PEG/LAP solution, and settled on and attached to the bottom of the plate, resulting in scaffolds with decreased cell concentrations in the upper layers. In addition, cells aggregated and formed large clumps that resulted in uneven cell distribution (data not shown). Similar phenomena were also reported previously [36, 39]. To overcome this, we sought to increase the density of the PEG/LAP to match the buoyant density of the cells. Percoll, composed of nano-level colloidal silica particles coated with polyvinylpyrrolidone (PVP), is non-cytotoxic [40] and has a long history of application in cell-based procedure. It was thus an apprporiate candidate agent for increasing the medium density. In our study, 37.5% Percoll (1.0496g/ml) successfully maintained uniform cell distribution in PEG/LAP solution or hydrogel after PSL. However, we found that Percoll also caused some unexpected extraneous photocrosslinking. Thus, the addition of Percoll in the fabrication of porous structures resulted in partial pore occlusion, caused by over- polymerized PEG, that we could observe using phase microscopy and also by fluorescently localizing the hADSCs trapped in the pores (Figure 6G, H). Future work is needed to test the application of other agents to increase the density of the PEG solution.

Cell viability is one of the key issues in the application of PSL technology to live cell-scaffold fabrication. The visible light we used here should have minimal effect on cell survival. Due to high free radical production efficiency of LAP, it is critical to protect cells from potential damage caused by the large amount of free radicals generated in a short period of time. It has been shown that selenium enhances the antioxidative capacity of the cells, preventing cell damage and death in bone marrow stromal cells in vitro [41]. Other studies also suggest that ITS, which contains selenium, improves cell growth in serum-free medium [42]. Therefore, we included ITS in the monomer solution in our study to further ensure cell survival. Compared to LSL that achieved about 65% cell viability after 7 days [36], our VL-PSL method dramatically increased cell survival. Because the PEGDA used here did not harbor any cell binding ligands, cells maintained a round morphology (Figures 6G & 7C). It has been shown that cell viability can be enhanced when RGD peptide are introduced to PEG hydrogels [36], suggesting the importance of extracellular ligands on cell survival and growth. In another ongoing study, we have successfully applied gelatin for live cell-scaffold construction using VL-PSL, which allowed cell binding and spreading in the biomaterial scaffold owning to the intrinsic ligand motifs of gelatin [10].

Finally, it has been shown that increased porosity of scaffolds promotes oxygenation of MSCs in alginate scaffolds and supports cell viability [43]. To test the effect of pore structure produced by VL-PSL on cell growth, we compared the level of cell metabolic activity (MTS assay) in solid or porous-1 structures at different time points. We postulated that an internal porous structure within scaffolds would increase the exchange of nutrients and oxygen, therefore enhancing cell growth. We did observe greater cell bioactivity in the porous scaffolds, despite some clumping of cells observed that occluded a number of pores as seen under phase contrast and fluorescence microscopy. Future studies will focus on optimization of Percoll-inclusive VL-PSL, and elucidation of the influence of different internal architecture produced by VL-PSL on stem cell growth and differentiation.

5. Conclusion

We report here the development of a VL-PSL technology for the fabrication of PEG hydrogels with custom-designed geometry and internal architecture, and the successful incorporation of live stem cells (hADSCs) within the scaffolds. hADSCs showed high viability in the fabricated scaffolds for up to 7 days post-encapsulation. Moreover, we observed that scaffolds with a porous interior structure better supported cellular metabolic activity than solid structures. The efficiency and effectiveness of the VL-PSL technology suggest its potential as a customizable approach to live cell-scaffold fabrication for in vitro tissue engineering and in vivo tissue repair.

Acknowledgments

Supported in part by a grant from the Commonwealth of Pennsylvania Department of Health, and by the National Institutes of Health (UL1 RR024153 and UL1TR000005).

References

[1]. Tuli R, Li WJ, Tuan RS. Current state of cartilage tissue engineering. Arthritis Res Ther. 2003; 5:235–8. [PubMed: 12932283]

[2]. Velema J, Kaplan D. Biopolymer-based biomaterials as scaffolds for tissue engineering. Adv Biochem Eng Biotechnol. 2006; 102:187–238. [PubMed: 17089791]

[3]. Hutmacher DW, Sittinger M, Risbud MV. Scaffold-based tissue engineering: rationale for computer-aided design and solid free-form fabrication systems. Trends Biotechnol. 2004; 22:354–62. [PubMed: 15245908]

[4]. Hollister SJ. Porous scaffold design for tissue engineering. Nat Mater. 2005; 4:518–24. [PubMed: 16003400]

[5]. Karageorgiou V, Kaplan D. Porosity of 3D biomaterial scaffolds and osteogenesis. Biomaterials. 2005; 26:5474–91. [PubMed: 15860204]

[6]. Yamane S, Iwasaki N, Kasahara Y, Harada K, Majima T, Monde K, et al. Effect of pore size on in vitro cartilage formation using chitosan-based hyaluronic acid hybrid polymer fibers. J Biomed Mater Res A. 2007; 81:586–93. [PubMed: 17177288]

[7]. Melchels FP, Feijen J, Grijpma DW. A review on stereolithography and its applications in biomedical engineering. Biomaterials. 2010; 31:6121–30. [PubMed: 20478613]

[8]. Yang S, Leong KF, Du Z, Chua CK. The design of scaffolds for use in tissue engineering. Part II. Rapid prototyping techniques. Tissue Eng. 2002; 8:1–11. [PubMed: 11886649]

[9]. Sinn DP, Cillo JE Jr. Miles BA. Stereolithography for craniofacial surgery. J Craniofac Surg. 2006; 17:869–75. [PubMed: 17003613]

[10]. Gauvin R, Chen YC, Lee JW, Soman P, Zorlutuna P, Nichol JW, et al. Microfabrication of complex porous tissue engineering scaffolds using 3D projection stereolithography. Biomaterials. 2012; 33:3824–34. [PubMed: 22365811]

[11]. Schuller-Ravoo S, Feijen J, Grijpma DW. Preparation of flexible and elastic poly(trimethylene carbonate) structures by stereolithography. Macromol Biosci. 2011; 11:1662–71. [PubMed: 22006829]

[12]. Seck TM, Melchels FP, Feijen J, Grijpma DW. Designed biodegradable hydrogel structures prepared by stereolithography using poly(ethylene glycol)/poly(D,L-lactide)-based resins. J Control Release. 2010; 148:34–41. [PubMed: 20659509]

[13]. Ikehata H, Ono T. The mechanisms of UV mutagenesis. J Radiat Res (Tokyo). 2011; 52:115–25. [PubMed: 21436607]

[14]. Leong KF, Chua CK, Sudarmadji N, Yeong WY. Engineering functionally graded tissue engineering scaffolds. J Mech Behav Biomed Mater. 2008; 1:140–52. [PubMed: 19627779]

[15]. Van Vlierberghe S, Dubruel P, Schacht E. Biopolymer-based hydrogels as scaffolds for tissue engineering applications: a review. Biomacromolecules. 2011; 12:1387–408. [PubMed: 21388145]

[16]. Fairbanks BD, Schwartz MP, Bowman CN, Anseth KS. Photoinitiated polymerization of PEG-diacrylate with lithium phenyl-2,4,6-trimethylbenzoylphosphinate: polymerization rate and cytocompatibility. Biomaterials. 2009; 30:6702–7. [PubMed: 19783300]

[17]. Ovsianikov A, Viertl J, Chichkov B, Oubaha M, MacCraith B, Sakellari I, et al. Ultra-low shrinkage hybrid photosensitive material for two-photon polymerization microfabrication. ACS Nano. 2008; 2:2257–62. [PubMed: 19206391]

[18]. Yurteri S, Onen A, Yagci Y. Benzophenone based addition fragmentation agent for photoinitiated cationic polymerization. Eur Polym J. 2002; 38:1845–50.

[19]. Ye GD, Kan WB, Yang JW, Zeng ZH, Liu XX. A study on hybrid oligomeric type II photoinitiator. E-Polymers. 2010; 138:1–16.

[20]. Dulay MT, Choi HN, Zare RN. Visible light-induced photopolymerization of an in situ macroporous sol-gel monolith. J Sep Sci. 2007; 30:2979–85. [PubMed: 17960846]

[21]. Neumann MG, Schmitt CC, Ferreira GC, Correa IC. The initiating radical yields and the efficiency of polymerization for various dental photoinitiators excited by different light curing units. Dent Mater. 2006; 22:576–84. [PubMed: 16289725]

[22]. Bryant SJ, Nuttelman CR, Anseth KS. Cytocompatibility of UV and visible light photoinitiating systems on cultured NIH/3T3 fibroblasts in vitro. J Biomat Sci-Polym E. 2000; 11:439–57.

[23]. Shi SQ, Nie J. A natural component as coinitiator for unfilled dental resin composites. J Biomed Mater Res B. 2007; 82B:44–50.

[24]. Rouillard AD, Berglund CM, Lee JY, Polacheck WJ, Tsui Y, Bonassar LJ, et al. Methods for Photocrosslinking Alginate Hydrogel Scaffolds with High Cell Viability. Tissue Eng Part C-Me. 2011; 17:173–9.

[25]. Castelvetro V, Molesti M, Rolla P. UV-curing of acrylic formulations by means of polymeric photoinitiators with the active 2,6-dimethylbenzoylphosphine oxide moieties pendant from a tetramethylene side chain. Macromol Chem Physic. 2002; 203:1486–96.

[26]. Kim SH, Chu CC. Visible light induced dextran-methacrylate hydrogel formation using (−)-riboflavin vitamin B2 as a photoinitiator and L-arginine as a co-initiator. Fiber Polym. 2009; 10:14–20.

[27]. Cruise GM, Hegre OD, Scharp DS, Hubbell JA. A sensitivity study of the key parameters in the interfacial photopolymerization of poly(ethylene glycol) diacrylate upon porcine islets. Biotechnol Bioeng. 1998; 57:655–65. [PubMed: 10099245]

[28]. Zorlutuna P, Annabi N, Camci-Unal G, Nikkhah M, Cha JM, Nichol JW, et al. Microfabricated Biomaterials for Engineering 3D Tissues. Adv Mater. 2012; 24:1782–804. [PubMed: 22410857]

[29]. Hsieh TM, Ng CW, Narayanan K, Wan AC, Ying JY. Three-dimensional microstructured tissue scaffolds fabricated by two-photon laser scanning photolithography. Biomaterials. 2010; 31:7648–52. [PubMed: 20667410]

[30]. Arcaute K, Mann B, Wicker R. Stereolithography of spatially controlled multi-material bioactive poly(ethylene glycol) scaffolds. Acta Biomater. 2010; 6:1047–54. [PubMed: 19683602]

[31]. Soletti L, Nieponice A, Guan J, Stankus JJ, Wagner WR, Vorp DA. A seeding device for tissue engineered tubular structures. Biomaterials. 2006; 27:4863–70. [PubMed: 16765436]

[32]. Spiller KL, Maher SA, Lowman AM. Hydrogels for the repair of articular cartilage defects. Tissue Eng Part B Rev. 2011; 17:281–99. [PubMed: 21510824]

[33]. Annabi N, Nichol JW, Zhong X, Ji C, Koshy S, Khademhosseini A, et al. Controlling the porosity and microarchitecture of hydrogels for tissue engineering. Tissue Eng Part B Rev. 2010; 16:371–83. [PubMed: 20121414]

[34]. Lin CC, Anseth KS. PEG hydrogels for the controlled release of biomolecules in regenerative medicine. Pharm Res. 2009; 26:631–43. [PubMed: 19089601]

[35]. Arcaute K, Mann BK, Wicker RB. Stereolithography of three-dimensional bioactive poly(ethylene glycol) constructs with encapsulated cells. Ann Biomed Eng. 2006; 34:1429–41. [PubMed: 16897421]

[36]. Chan V, Zorlutuna P, Jeong JH, Kong H, Bashir R. Three-dimensional photopatterning of hydrogels using stereolithography for long-term cell encapsulation. Lab Chip. 2010; 10:2062–70. [PubMed: 20603661]

[37]. Williams CG, Malik AN, Kim TK, Manson PN, Elisseeff JH. Variable cytocompatibility of six cell lines with photoinitiators used for polymerizing hydrogels and cell encapsulation. Biomaterials. 2005; 26:1211–8. [PubMed: 15475050]

[38]. Hill-West JL, Chowdhury SM, Slepian MJ, Hubbell JA. Inhibition of thrombosis and intimal thickening by in situ photopolymerization of thin hydrogel barriers. Proc Natl Acad Sci U S A. 1994; 91:5967–71. [PubMed: 8016098]

[39]. Dhariwala B, Hunt E, Boland T. Rapid prototyping of tissue-engineering constructs, using photopolymerizable hydrogels and stereolithography. Tissue Eng. 2004; 10:1316–22. [PubMed: 15588392]

[40]. Wakefield JS, Gale JS, Berridge MV, Jordan TW, Ford HC. Is Percoll innocuous to cells? Biochem J. 1982; 202:795–7. [PubMed: 6284138]

[41]. Ebert R, Ulmer M, Zeck S, Meissner-Weigl J, Schneider D, Stopper H, et al. Selenium supplementation restores the antioxidative capacity and prevents cell damage in bone marrow stromal cells in vitro. Stem Cells. 2006; 24:1226–35. [PubMed: 16424399]

[42]. Bottenstein J, Hayashi I, Hutchings S, Masui H, Mather J, McClure DB, et al. The growth of cells in serum-free hormone-supplemented media. Methods Enzymol. 1979; 58:94–109. [PubMed: 423795]

[43]. Fedorovich NE, Kuipers E, Gawlitta D, Dhert WJ, Alblas J. caffold porosity and oxygenation of printed hydrogel constructs affect functionality of embedded osteogenic progenitors. Tissue Eng Part A. 2011; 17:2473–86. [PubMed: 21599540]

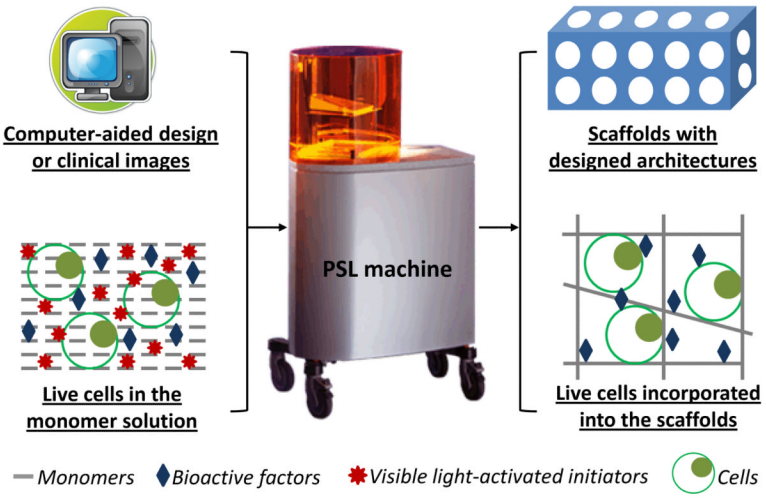

Figure 1.

Diagrammatic scheme of the visible light-based projection stereolithography (VL-PSL) system with live cell fabrication capability. Computer-aided design (CAD) was used to produce 3D models with desired architectures. Designed models were then sliced into a series of 2D images which were transferred to the PSL device. By sequential photocrosslinking, 3D scaffolds were built which were exact replicas of designed 3D models. Meanwhile, live cells evenly mixed in the monomer solution were uniformly incorporated within the scaffolds. During the process, visible light was used to avoid potential damage of UV damage of cells.

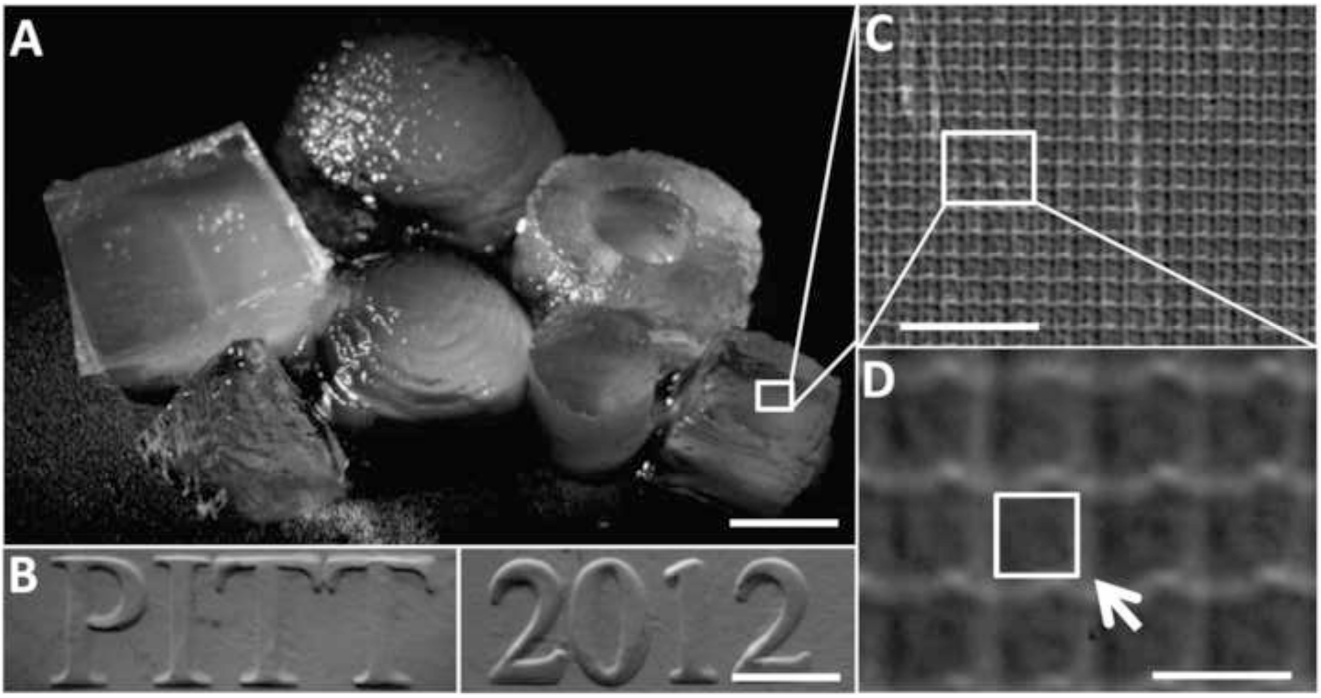

Figure 2.

PEG hydrogels scaffolds produced by VL-PSL. (A) PEG hydrogels with cubical, spherical, cylindrical and pyramidal shapes. (B) Alphanumeric stereo characters (PITT and 2012) made from PEG hydrogel. (C, D) Typical surface texture of VL-PSL manufactured PEG hydrogels on which voxel structures were observed. The dimension of one voxel (whites square indicated by the arrow in D) was 68-73 μm × 68-73 μm (width × length). The PEG concentration used here was 10% (w/v in water) and LAP concentration was 0.5% (w/v). Bar in A, B, C, D = 5 mm, 1 mm, 500 μm and 100 μm, respectively.

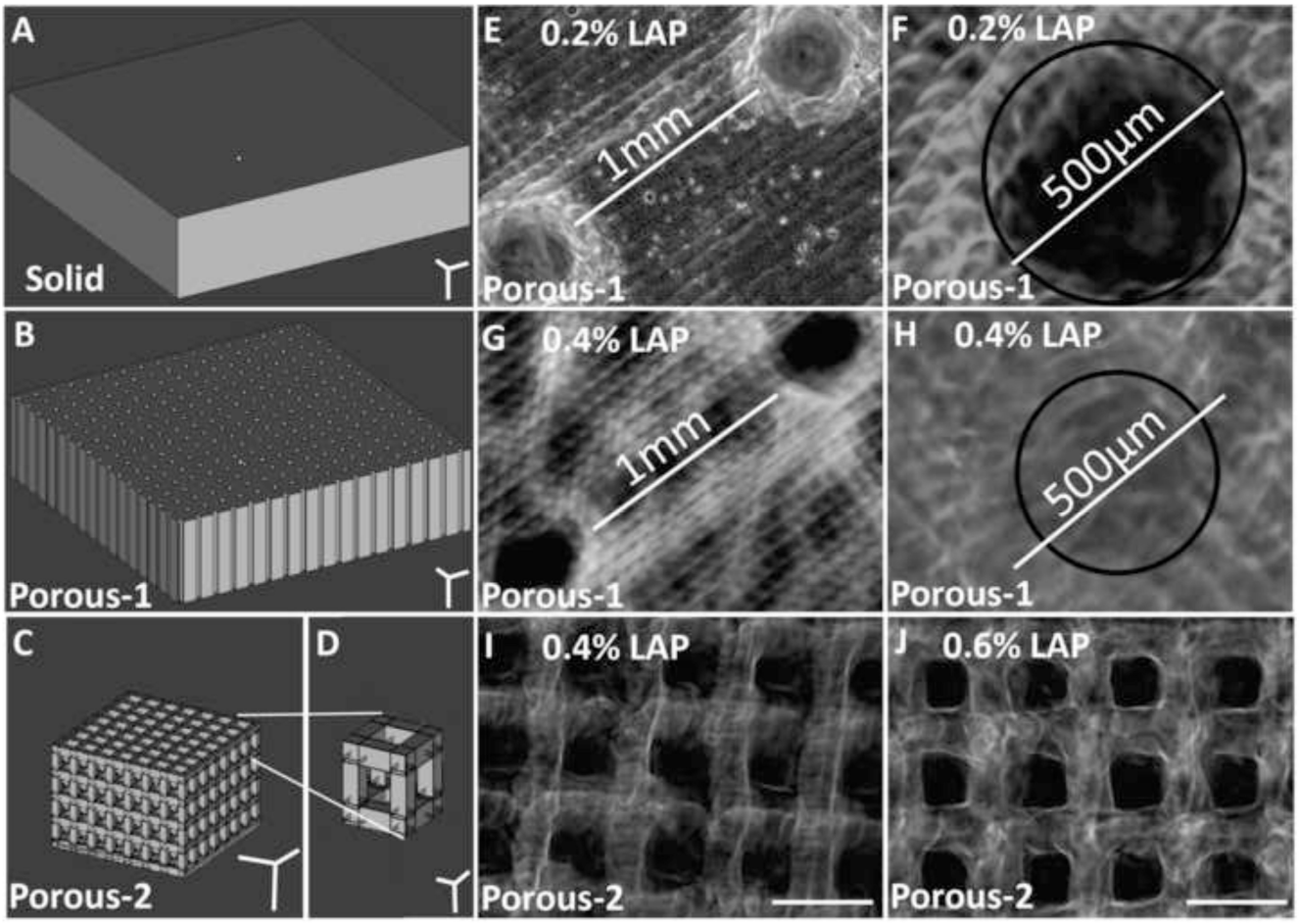

Figure 3.

Fidelity evaluation of VL-PSL fabrication using different LAP concentrations. (A-D) 3D models designed by Magics 14 software for (A) solid, (B) uniaxial (porous-1) and (C, D) biaxial (porous-2) porous structures. (E-H) The internal architectures of porous-1 PEG hydrogels produced with different initiator concentrations (E, F: 0.2%; G, H: 0.4%). The distance between 2 neighboring tubes was indicated by the white lines in E and G. Black circles in F and H indicate the approximate inner surface of the pores in porous-1 structures. The dimensions of the intended pore diameter of these structures were indicated by white lines, revealing the differences in fidelity of the photocrosslinking using different LAP concentration. (I, J) The internal architectures of porous-2 PEG hydrogels produced with different initiator concentrations (I: 0.4%; J: 0.6%). 0.4% LAP failed to build intact structure and 0.6% LAP was capable to reproduce the structure. Bar in A, B = 2 mm. Bar in C = 1 mm. Bar in D = 200 μm. Bar in E, G = 1 mm. Bar in F, H, I and J = 500 μm.

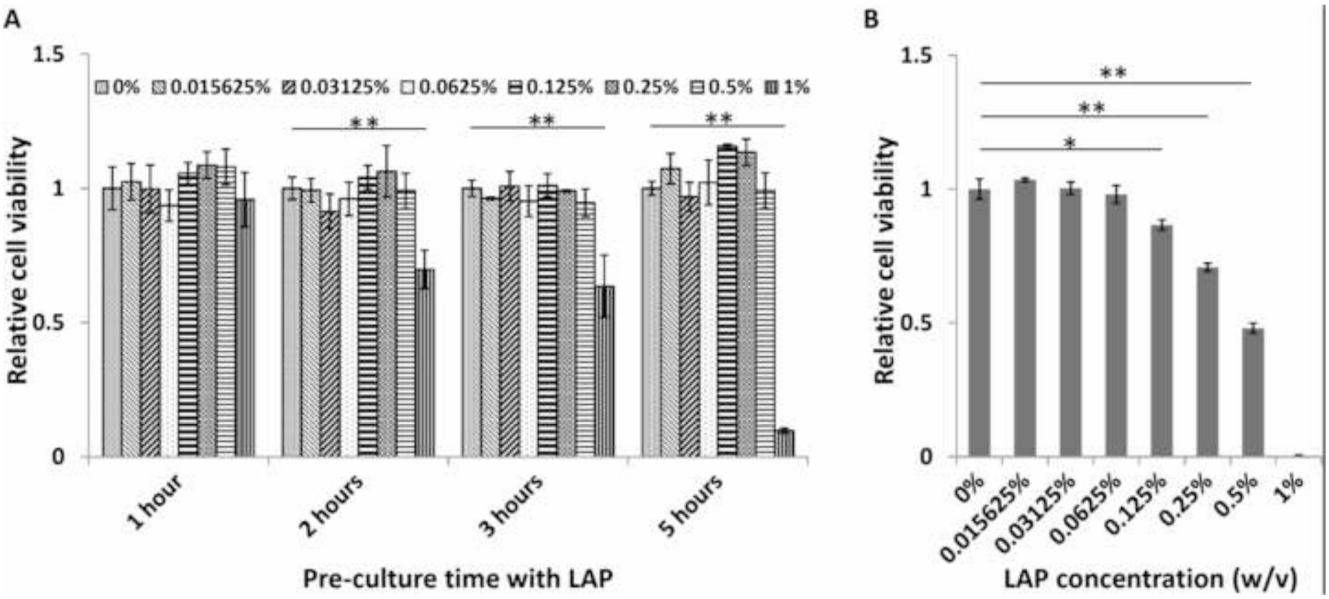

Figure 4.

Cytotoxicity test of LAP. (A) MTS assay of hADSCs treated with different concentrations of LAP in HBSS for different times followed by culture in GM for 3 days after LAP removal. All MTS assay results were normalized to those in the group without LAP treatment (set as 1) at different time. (B) MTS assay of hADSCs cultured in GM with different concentrations of LAP for 3 days. All values are mean ± SD; $p<0.05$(*) and $p<0.01$(**).

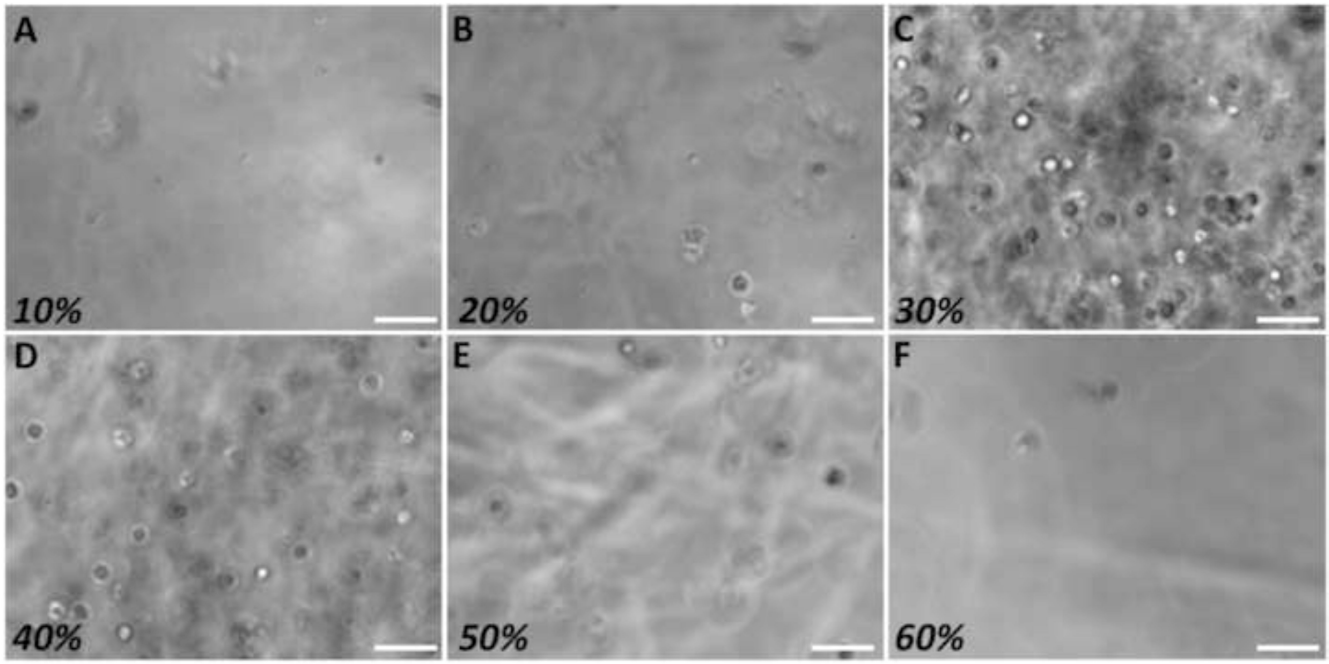

Figure 5.
Optimal medium density as adjusted by Percoll for suspension of hADSCs in PEG solution. Keeping PEG concentration at 10% (w/v), a discontinuous Percoll gradient was made ranging from 10% to 90% Percoll in HBSS (v/v). A-F showed cell distribution in the 10%-60% Percoll layers. The greatest number of ADSCs was seen in the layers with 30% and 40% Percoll. Bar = 100 μm.

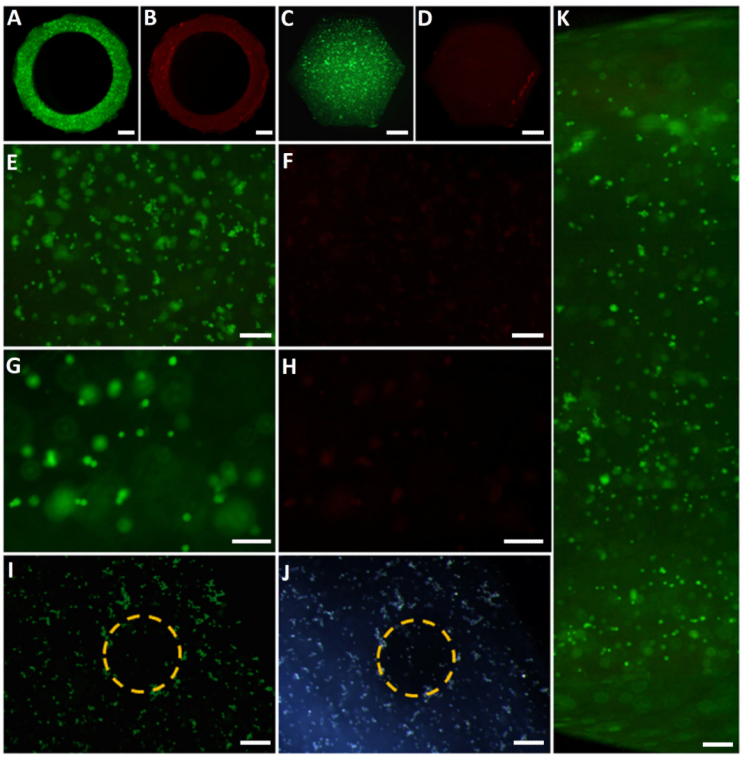

Figure 6.

hADSCs viability in VL-PSL built PEG scaffolds 24 hours after fabrication.(A, C, E, G, I, K) Calcein-AM staining (Green = Live cells) and (B, D, F, H) EthD-1 staining (Red = Dead cells) in (A, B) ring, (C, D) hexagonal and (E-H) solid scaffolds, showed that most encapsulated cells were alive 24 hours after VL-PSL. (I, J) Pore structure in porous-1 structure shown under (I) fluorescence microscopy with calcein-AM staining and (J) bright-field microscopy. The intended dimension of the 500 μm pore is superimposed upon the image with a yellow dashed circle. (K) Lateral view of the full thickness of a 5 mm high solid scaffold stained with calcein-AM showing high cell viability and uniform distribution through the depth of the construct. Bars in A, B, C, D, E, F, I, J and K = 200 μm. Bars in G, H =100 μm.

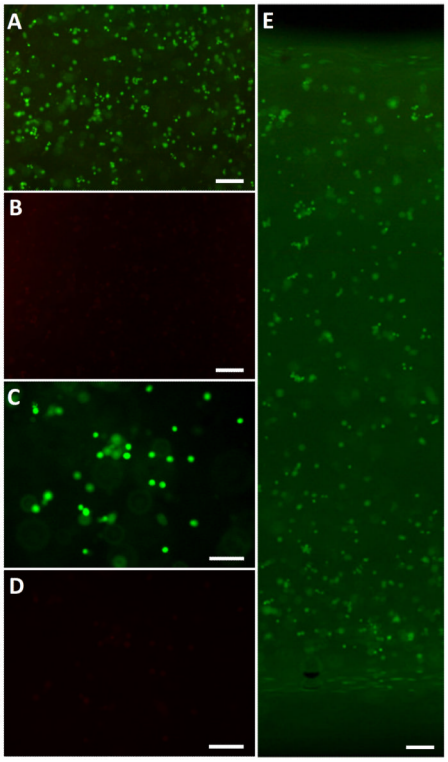

Figure 7.
hADSCs viability in solid VL-PSL built constructs on culture day 7 in growth medium after fabrication. (A, C, E) Calcein-AM staining and (B, D) EthD-1 staining. (E) Lateral view of Calcein-AM stained cells in a solid scaffold 7 days after fabrication revealing continuous high cell viability and uniform cell distribution through the depth of the construct. Bars in A, B, E = 200 μm. Bars in C, D, = 100 μm.

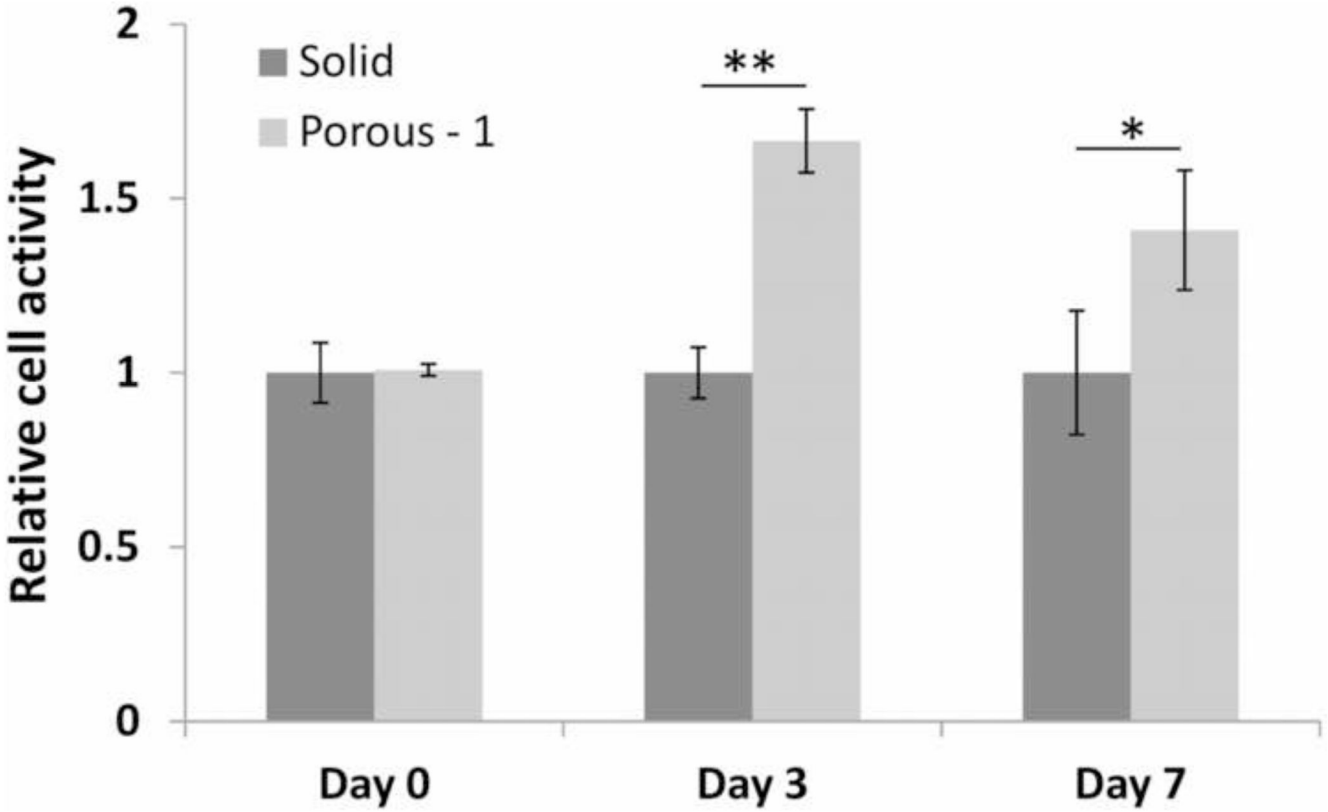

Figure 8.

MTS analysis of metabolic activity of PEG-encapsulated hADSCs in solid and porous-1 constructs at day 0, 3 and 7 after fabrication. All MTS results in porous-1 groups were normalized to those in solid groups (set as 1). On day 0, cell viability was statistically equivalent. At day 3 and 7, porous group exhibited higher cell activity or viability than solid scaffolds. All values are mean ± SD; $p<0.05$(*) and $p<0.01$(**).

Table 1

Screening of potential visible light-activated initiators for live cell-fabrication using PSL apparatus under visible light mode.

Candidate initiators	Ref.	Solubility in water ?	Gelation under visible light mode?
4,4′-Bis(diethylamino)benzophenone	[17]	No	N/A
4-(dimethylamino)benzophenone	[18]	No	N/A
4,4′-bis(dimethylamino)benzophenone	[19]	No	N/A
Bis(cyclopenta-l,3-diene)bis(l-(2,4-difluorophenyl)-3H-pyrrol-3-yl)titanium(Irgacure 784)	[20]	No	N/A
Phenylbis(2,4,6-trimethylbenzoyl)phosphine oxide (Irgacure 819)	[21]	No	N/A
Ethyl (2,4,6-trimethylbenzoyl) phenyl phosphinate (Lucirin TPO-L)	[21]	No	N/A
Camphorquinone/ethyl 4-N,N-dimethylaminobenzoate	[22,23]	No	N/A
2,2-Dimethoxy-2-phenylacetophenone (Irgacure 651)	(22]	Limited	No
2/2′-Azobis[2-methyl-N-(2-hydroxyethyl)propionamide] (VA-086)	[24]	Yes	No
2-hydroxY-l-[4-(hydroxyethoxy)phenyl]-2-methvl-l-propanone (Irgacure 2959)	[16,22]	Yes	No
Diphenyl(2,4,6-trimethylbenzoyl)phosphine oxide (Darocur TPO)	[25]	Limited	Some
Riboflavin/Triethanolamine/l-vinyl-2-pyrrolidinone	[26,27]	Yes	No
Eosin Y/Triethanolamine/l-vinyl-2-pyrrolidinone	[27]	Yes	Some
Lithium phenyl-2,4,6-trimethylbenzoylphosphinate (LAP)	[16]	Yes	Yes